Brief Communication

Visualization of Synaptic Ca^{2+}/Calmodulin-Dependent Protein Kinase II Activity in Living Neurons

Keizo Takao,[1,2,3] Ken-Ichi Okamoto,[1] Terunaga Nakagawa,[1] Rachael L. Neve,[5] Takeharu Nagai,[4] Atsushi Miyawaki,[4] Tsutomu Hashikawa,[3] Shigeo Kobayashi,[2] and Yasunori Hayashi[1]

[1]RIKEN–Massachusetts Institute of Technology (MIT) Neuroscience Research Center, The Picower Center for Learning and Memory, Department of Brain and Cognitive Sciences, MIT, Cambridge, Massachusetts 02139, [2]Division of Biological Information, Department of Intelligence Science and Technology, Graduate School of Informatics, Kyoto University, Kyoto 606-8501, Japan, [3]Laboratory for Neural Architecture and [4]Laboratory for Cell Function Dynamics, Advanced Technology Development Group, Brain Science Institute, RIKEN, Saitama 351-0198, Japan, and [5]Department of Psychiatry, Harvard Medical School, MRC 223, McLean Hospital, Belmont, Massachusetts 02478

Ca^{2+}/calmodulin-dependent protein kinase II (CaMKII) is highly enriched in excitatory synapses in the CNS and critically involved in synaptic plasticity, learning, and memory. However, the precise temporal and spatial regulation of CaMKII activity in living cells has not been well described, because of a lack of specific methods. We tried to address this by optically detecting the conformational change in CaMKII during activation using fluorescence resonance energy transfer (FRET). The engineered FRET probe Camuiα detects calmodulin binding and autophosphorylation at threonine 286 that renders the enzyme constitutively active. In combination with two-photon microscopy, we demonstrate that Camuiα can be used to observe temporal and spatial regulation of CaMKII activity in living neurons.

Key words: **Ca^{2+}/calmodulin-dependent protein kinase II; fluorescent resonance energy transfer; two-photon laser-scanning microscopy; synaptic plasticity; hippocampus; excitatory amino acid**

Introduction

Ca^{2+} influx via postsynaptic NMDA receptors triggers the activation of Ca^{2+}/calmodulin-dependent protein kinase II (CaMKII), followed by a series of autophosphorylation events catalyzed by both intersubunit and intrasubunit reactions. This property, which enables activated CaMKII to stay activated until all subunits are dephosphorylated, has been suggested as an underlying mechanism for long-term potentiation (LTP), a persistent increase in synaptic efficacy (Hudmon and Schulman, 2002; Lisman et al., 2002). Elevated CaMKII activity likely remodels the postsynaptic protein complex, leading eventually to the insertion of new AMPA receptors at the surface of dendritic spines and to the enhancement of synaptic transmission (Shi et al., 1999; Hayashi et al., 2000). Although this model is widely accepted, because of technical difficulty, surprisingly few studies have confirmed constitutive activation of CaMKII after LTP induction (Fukunaga et al., 1995; Ouyang et al., 1997). Furthermore, although CaMKII is involved in various neuronal events, including synapse and spine formation, dendritic maturation, and cellular processes such as cell-cycle regulation, gene expression, and apoptosis (Hudmon and Schulman, 2002; Lisman et al., 2002), information on spatial and temporal patterns of CaMKII activation in living cells is lacking. In view of this, we designed an approach to optically monitor CaMKII activity by detecting conformational changes in CaMKII associated with its activation using fluorescence resonance energy transfer (FRET) technology (Miyawaki et al., 1997; Zhang et al., 2002). In combination with two-photon laser-scanning microscopy, we could visualize CaMKII activation induced by glutamate receptor activation in dendrites and spines.

Received Sept. 9, 2003; revised Feb. 7, 2005; accepted Feb. 8, 2005.

K.T. is a recipient of the Special Postdoctoral Researchers Fellowship from RIKEN and is partly supported by the Nakayama Foundation for Human Science. T.N. is a recipient of a long-term fellowship from the Human Frontier Science Program. Y.H. is supported in part by The Ellison Medical Foundation. We thank Drs. Atsuhiko Ishida, Satoshi Kida, Alcino Silva, Show-ming Sally Kwok, Nasheed Jamal, Shan Riku, Kaoru Endo, Koichi Takahashi, and Travis Emery for valuable advice and sharing of resources.

Correspondence should be addressed to Dr. Yasunori Hayashi, RIKEN–MIT Neuroscience Research Center, The Picower Center for Learning and Memory, Department of Brain and Cognitive Sciences, MIT, 77 Massachusetts Avenue E18-270, Cambridge, MA 02139. E-mail: yhayashi@mit.edu.

DOI:10.1523/JNEUROSCI.0085-05.2005

 0270-6474/05/253107-06$15.00/0

Materials and Methods

Molecular biology and biochemistry. Camuiα (GenBank accession number AY928551) was constructed from rat CaMKIIα and improved versions of both yellow fluorescent protein (YFP), with less pH sensitivity, rapid fluorophore formation, and better brightness (Venus) (Nagai et al., 2002), and cyan fluorescent protein (CFP), with better brightness (S175G mutation) (T. Nagai and A. Miyawaki, unpublished observations). The construct was subcloned into baculovirus expression vector pTriplEx-4 (Novagen, Madison, WI) or pBacPAK9 (Clontech, Palo Alto, CA) and cotransfected into Sf21 cells with BacVector 1000 DNA (Novagen) to obtain baculovirus particles. Sf21 or BTI-Tn-5B1–4 cells were infected with the virus and recovered after 36–48 h. The Camuiα was affinity-purified by calmodulin–Sepharose 4B (Amersham Biosciences, Piscataway, NJ) according to the protocol of the manufacturer and then gel filtrated through Sephacryl S-300 (Amersham Biosciences) in CaMKII assay buffer containing 40 mM HEPES-Na, pH 8.0, 0.1 mM EGTA, 5 mM magnesium acetate, 0.01% Tween 20, and 1 mM DTT (Katoh and Fuji-

sawa, 1991). This resulted in the removal of endogenous ATP, calmodulin, and other contaminants reactive to CaMKII and green fluorescent protein (GFP) antibodies. To stimulate Camuiα, Ca^{2+} (0.2 mM total, ~0.1 mM free) was added in the presence of 1 μM calmodulin and 50 μM ATP, unless otherwise specified, at room temperature. The reaction was stopped by 0.4 mM EGTA. There was some variation in the basal FRET level as well as in the magnitude of change induced by Ca^{2+} among different purified preparations. We therefore compared absolute FRET signal only within the same set of experiments. For expression in human embryonic kidney 293T (HEK293T) cells, Camuiα was transfected by a liposome-mediated method. After 2–3 d, the cells were homogenized in CaMKII assay buffer. After centrifugation, the supernatant was used as the source of the enzyme. To estimate the size of undenatured oligomer, this supernatant was separated with a Superdex 200 column (Amersham Biosciences). For fluorospectrometric measurement of FRET, CFP was specifically excited at 433 nm. FRET level is expressed throughout as a ratio of emissions at 478 nm (CFP) to 525 nm (YFP), in which a higher value indicates less FRET. Autophosphorylation of CaMKII was detected by [γ-^{32}P]ATP (~1000 cpm/pmol) incorporation or Western blotting with anti-phospho-T286 (Upstate Biotechnology, Lake Placid, NY) and anti-phospho-T305/T306 CaMKIIα (Elgersma et al., 2002) antibodies. Herpes virus expression vector was generated as described previously (Carlezon et al., 2000). Kinase reactions were performed as described previously, using syntide-2 as a substrate for 1 min at room temperature (Katoh and Fujisawa, 1991; Hayashi et al., 2000).

Imaging. FRET imaging using a two-photon laser-scanning microscope and subsequent analyses were performed as described previously (Okamoto et al., 2004). HeLa cells were transfected with cDNA as described above and imaged 2–4 d later in solution containing the following (in mM): 129 NaCl, 5 KCl, 2 $CaCl_2$, 1 $MgCl_2$, 30 glucose, and 25 HEPES-Na, pH 7.4. The cells were stimulated with a 5 μM concentration of the calcium ionophore 4-bromo-A23187 (4-Br-A23187) (A.G. Scientific, San Diego, CA), a nonfluorescent derivative of A23187. Hippocampal-dissociated cultures were prepared as described previously (Renger et al., 2001). Neurons were transfected by the Ca^{2+}-phosphate method (at 7–11 d *in vitro*) or infected by herpes virus expression vector (at 13 d *in vitro*) and imaged at 14–16 d *in vitro* in solution containing the following (in mM): 145 NaCl, 3 KCl, 1.2 $CaCl_2$, 1.2 $MgCl_2$, 10 glucose, and 10 HEPES-Na, pH 7.4.

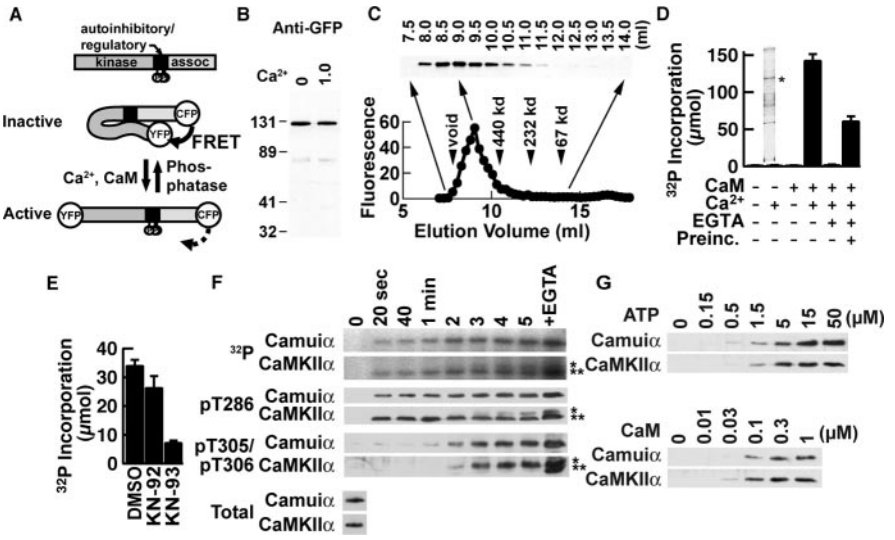

Figure 1. Biochemical characterization of Camuiα. ***A***, Structure of Camuiα. assoc, Association domain; P, major autophosphorylation sites. ***B***, Western blotting with an anti-GFP antibody in the absence and presence of Ca^{2+} (1 mM). ***C***, Estimation of the size of the holoenzyme of Camuiα by gel filtration. An anti-GFP immunoblot of fractions is shown at the top. YFP fluorescence of each fraction is plotted at the bottom. ***D***, Kinase activity of Camuiα expressed and partially purified from Sf21 cells with syntide-2 as substrate. Preinc., Preincubation with Ca^{2+} before addition of EGTA and syntide-2. Inset, Silver staining of representative preparation. The asterisk corresponds to the molecular mass of Camuiα. ***E***, Inhibition of kinase activity by 5 μM KN-93 but not by the inactive analog KN-92. Calmodulin (0.1 μM) was used. ***F***, Time course of autophosphorylation of Camuiα and CaMKIIα. EGTA was added after obtaining 5 min of sample, and the reaction was further proceeded for 2 min. Total autophosphorylation was detected using an autoradiogram of ^{32}P-incorporated proteins. Site-specific phosphorylation was detected with antibodies specific for phosphorylated T286 or T305/T306. Total amounts of Camuiα and CaMKIIα detected by anti-CaMKII antibody are also shown. A single asterisk indicates the original molecular mass; double asterisks indicate the gel-shifted population. ***G***, Concentration requirement of ATP and calmodulin of Camuiα and CaMKIIα for activation detected by an antibody against phosphorylated T286. Error bars represent SEM.

Results

Design and biochemical characterization of the FRET-based reporter for CaMKII activation, Camuiα

At basal cellular Ca^{2+} concentrations, CaMKII is kept inactive by an autoinhibitory domain that masks the catalytic core of the enzyme (Goldberg et al., 1996; Hudmon and Schulman, 2002; Lisman et al., 2002). The binding of the Ca^{2+}/calmodulin complex to the calmodulin-binding domain induces a conformational change in the enzyme to prevent this interaction, thereby exposing the kinase domain to substrates. Once activated, the kinase autophosphorylates T286 in the autoinhibitory domain of the adjacent subunit, which unmasks the catalytic core and makes the kinase constitutively active. Because these processes involve conformational changes in the protein, we speculated that, by flanking the entire CaMKII protein with YFP and CFP and monitoring FRET between these two fluorophores, we could image the CaMKII activation process (Fig. 1*A*).

The engineered protein Camuiα had an expected molecular mass of 110 kDa on Western blotting (Fig. 1*B*). The undenatured holoenzyme was eluted in a single peak with a molecular mass of >1000 kDa on gel filtration, indicating oligomer formation (Fig. 1*C*). Camuiα was then expressed in insect cells and partially purified (Fig. 1*D*, inset). When kinase activity was measured using syntide-2 as a substrate, Camuiα had kinase activity triggered by Ca^{2+} and calmodulin (Fig. 1*D*). In the presence of EGTA, Ca^{2+} failed to trigger kinase activity. When EGTA was added after Camuiα was preincubated with Ca^{2+} and calmodulin in the absence of syntide-2 for 1 min, EGTA only partially blocked kinase activity, indicating that Camuiα had become a Ca^{2+}-independent, constitutively active form, like wild-type CaMKII. This activation was also abolished by KN-93, a specific inhibitor of the calmodulin–CaMKII interaction, but not by KN-92, an inactive analog, confirming the specific involvement of binding between calmodulin and the CaMKII moiety of Camuiα (Fig. 1*E*).

Because autophosphorylation is a major regulatory mechanism of CaMKII, we determined the time course of total phosphorylation using [γ-^{32}P]ATP and site-specific phosphorylations using specific antibodies against phosphorylations at T286 and T305/T306 to compare the autophosphorylation of Camuiα with that of wild-type CaMKII (Fig. 1*F*) (Ouyang et al., 1997; Elgersma et al., 2002). Incorporation of ^{32}P into wild-type CaMKII was detected 20 s after the addition of Ca^{2+} and gradually increased. The site-specific antibodies revealed that phosphorylation at T286 occurs immediately after stimulation and is sustained, whereas the phosphorylation at T305/T306 gradually

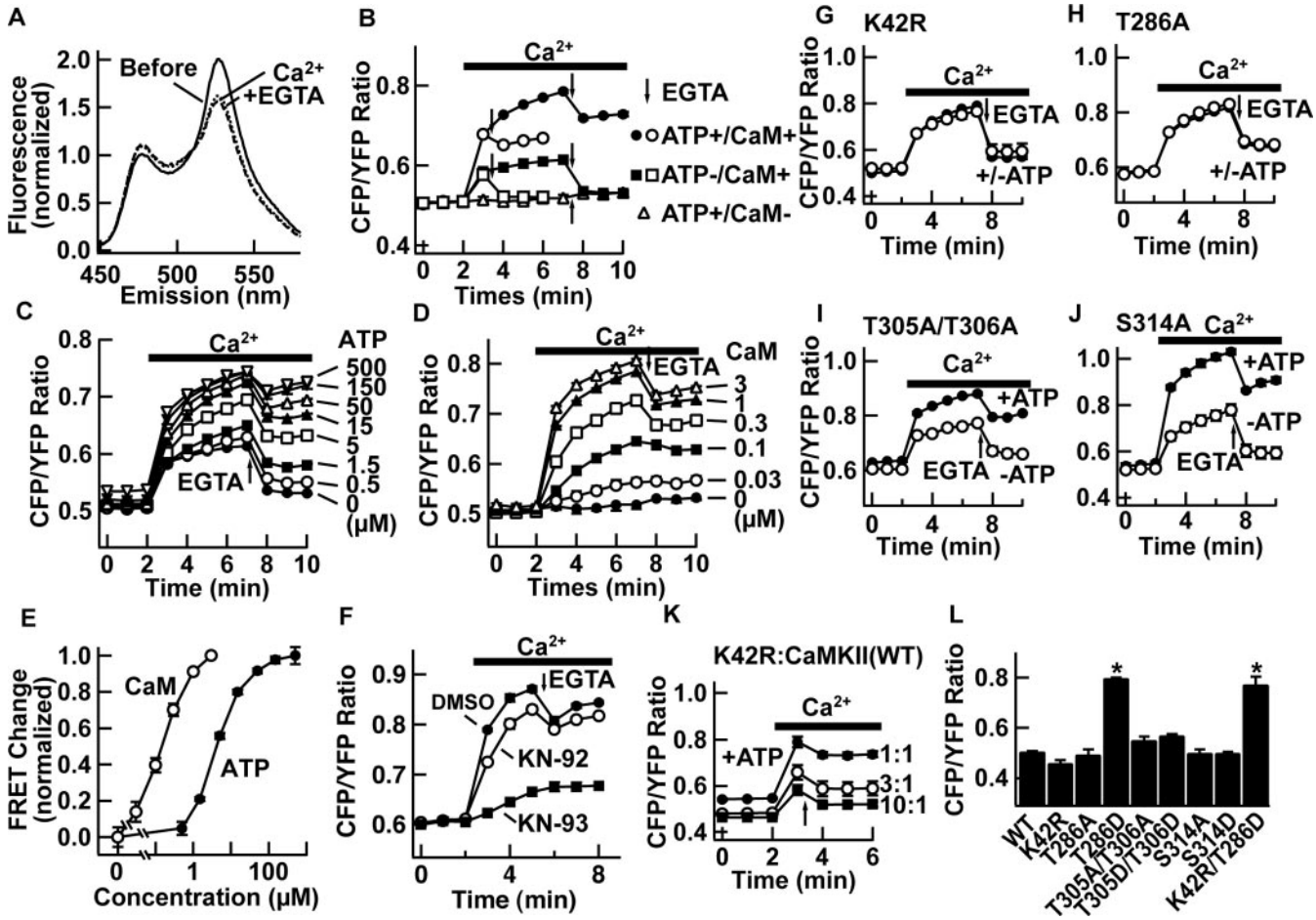

Figure 2. Characterization of FRET of Camuiα in cell lysate. ***A***, Emission fluorescence spectra of Camuiα after CFP-specific excitation before (solid line) and after (dashed line) addition of Ca^{2+}. Further addition of EGTA did not reverse the effect (dotted line). ***B***, Representative experiment of time course of FRET change in the presence or absence of ATP and calmodulin. EGTA was added where indicated by arrows (1 or 5 min after addition of Ca^{2+}). ***C–E***, Concentration dependency of ATP and calmodulin. ***E***, Normalized response after a 5 min reaction. In the absence of calmodulin, EGTA slightly increased the ratio, but this seemed to be unrelated to a chelating effect, because such an increase was observed even in the absence of Ca^{2+} (data not shown). ***F***, Inhibition of FRET change by KN-93 (5 μM) but not by KN-92 (5 μM). Calmodulin (0.1 μM) was used. ***G–J***, FRET response of Camuiα mutants after the addition of Ca^{2+} and after chelation. Response was compared in the presence (filled circles) and absence (open circles) of ATP. ***K***, FRET response of kinase-null (K42R) Camuiα coexpressed with increasing ratio of untagged wild-type CaMKII. ***L***, Effect of mutations of basal-level FRET ($n = 3$ each). *$p < 0.01$; ANOVA. Experiments were done with partially purified enzymes from insect cells (***A–J***) or with a HEK293T cell homogenate (***K, L***). Error bars represent SEM.

increases after 2 min and stabilizes after 3 min. After the addition of EGTA, the resulting removal of the Ca^{2+}/calmodulin complex from CaMKII unmasks the calmodulin-binding domain and induces additional phosphorylation, especially at T305/T306. The activation of Camuiα follows an essentially similar time course. In addition, the ATP and calmodulin concentration dependencies of Camuiα and CaMKII, as assessed by T286 phosphorylation, were also parallel (Fig. 1*G*). The autophosphorylation of Camuiα at T286 also suggests that Camuiα forms a functional oligomer similar to the wild-type enzyme, because this reaction occurs via intersubunit, but not intrasubunit, reactions within an oligomer (Mukherji and Soderling, 1994). In summary, these results indicate that Camuiα retains the regulatory mechanisms as CaMKII.

Camuiα shows FRET that responds to Ca^{2+}

We next tested, by fluorospectrometric assay, whether Camuiα shows FRET (Fig. 2). After CFP-specific excitation, Camuiα exhibited both YFP and CFP peaks, indicating that FRET occurs between the fluorophores at each end of the CaMKII (Fig. 2*A*). The YFP signal disappeared by limited protease digestion with a concomitant dequenching of the CFP signal, whereas the integrity of the YFP molecule itself was confirmed by YFP fluorescence before and after at YFP excitation (data not shown).

To test whether activation of Camuiα induces changes in FRET efficiency, we added Ca^{2+} to Camuiα in the presence of ATP and calmodulin and monitored the emission spectra (Fig. 2*A*,*B*). The addition of Ca^{2+} decreased FRET efficiency or, conversely, increased the CFP/YFP ratio. This FRET change persisted even after the addition of EGTA (Fig. 2, arrows), indicating that the FRET change reflects a constitutive activation of CaMKII. Ca^{2+} added after introduction of EGTA failed to induce a change in FRET (data not shown). The decrease in FRET was not attributable to degradation of the protein, because the molecular mass remained the same on Western blot (Fig. 1*B*,*F*,*G*). The half-maximum concentration for activation was ~4 μM for ATP and ~130 nM for calmodulin, a range similar to previously reported numbers for wild-type CaMKIIα (Fig. 2*C–E*) (Colbran, 1993; De Koninck and Schulman, 1998).

FRET change in Camuiα detects calmodulin binding and T286 phosphorylation

Which step of the CaMKII activation process does the FRET change reflect? Ca^{2+} had little effect when calmodulin was omit-

ted from the reaction (Fig. 2*B*,*D*). Inclusion of KN-93 or mutation of T305/T306 into aspartic acid (T305D/T306D; numbering based on CaMKIIα), which abolishes calmodulin binding, entirely eliminated FRET change (Fig. 2*F* and data not shown). In contrast, when the kinase reaction was prevented by omitting ATP or mutating a catalytically critical amino acid (K42R), FRET still changed with the addition of Ca^{2+}, but to a lesser extent (Fig. 2*C*,*G*). More importantly, after chelating of Ca^{2+} with EGTA, the FRET change decreased toward the baseline (Fig. 2*B*,*C*,*G*). These results indicate that both binding of calmodulin and autophosphorylation can induce conformational changes in Camuiα that lead to FRET decrease.

We then tested the necessity of autophosphorylation at T286 for a persistent change in FRET after removal of Ca^{2+}/calmodulin. A mutation of T286 into alanine (T286A) abolished the ATP-dependent component of FRET change (Fig. 2*H*). In contrast, with alanine mutations at T305/T306 and S314, both located in the calmodulin-binding domain, we could induce persistent ATP-dependent FRET change, indicating that phosphorylations of these sites are not major contributors to conformational change (Fig. 2*I*,*J*).

We next wanted to test whether the autophosphorylation at T286 is sufficient by itself to cause FRET change. We addressed this with two experiments. First, we used the fact that phosphorylation at T286 is catalyzed between adjacent subunits, whereas other phosphorylations such as T305/T306 are catalyzed within the subunit (Mukherji and Soderling, 1994). Thus, if Camuiα with K42R mutation is coexpressed with wild-type, untagged CaMKIIα, the Camuiα–K42R will be phosphorylated at T286 by an intersubunit reaction with an adjacent wild-type subunit, but phosphorylations typically mediated by intrasubunit reactions at other sites on Camuiα–K42R will not take place. We also limited the reaction time to 1 min, when phosphorylation is mostly limited to T286 (Fig. 1*F*). In this way, we expected that we would see the specific effect of T286 phosphorylation on FRET change. Camuiα–K42R by itself did not show ATP-dependent FRET change (Fig. 2*G*). However, by increasing the ratio of untagged wild-type enzyme versus Camuiα–K42R, FRET showed a larger change in response to stimulation with Ca^{2+}, and, in addition, we observed a persistent change after chelating Ca^{2+} (Fig. 2*K*).

In the second experiment, we compared unstimulated FRET levels in Camuiα with mutations at T286, T305/T306, and S314 (Fig. 2*L*). If phosphorylation of T286 is sufficient to change FRET, the aspartate mutation at T286 (T286D), which mimics phosphorylated status (Brickey et al., 1994), should induce FRET change without stimulation. We found that the T286D mutation changed FRET significantly, whereas other aspartate or alanine mutants did not. We were, however, concerned that T286D mutation may induce secondary phosphorylation at other sites. Therefore, we made double-mutant K42R+T286D, which abolished kinase activity but still mimicked phosphorylation at T286. This mutant showed a comparable change to T286D, indicating that autophosphorylation at T286 itself is sufficient for FRET change.

In sum, our results are consistent with the idea that FRET changes mostly detect calmodulin binding and phosphorylation at T286.

Imaging of Camuiα activation in HeLa cells

Subsequently, to test whether we can see Ca^{2+}-induced FRET change in living cells, we observed HeLa cells expressing Camuiα by two-photon laser-scanning microscopy (Fig. 3). After CFP-specific excitation, we detected signals in both CFP and YFP

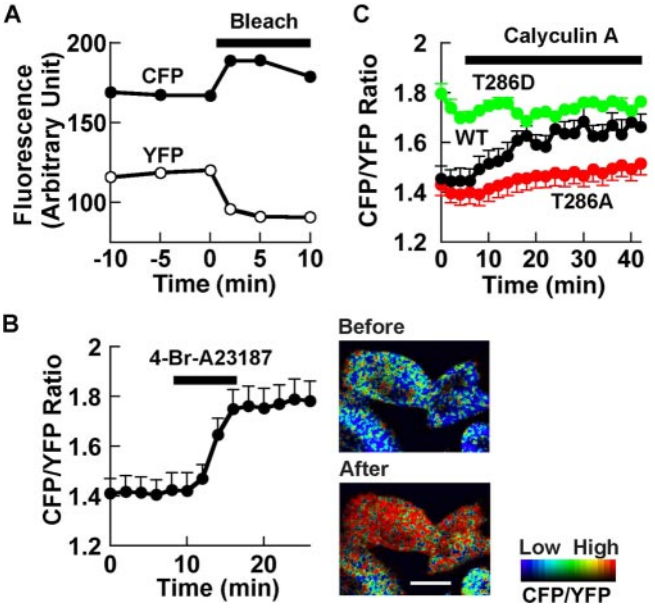

Figure 3. Characterization of FRET of Camuiα in HeLa cells with two-photon laser-scanning microscopy. ***A***, Acceptor bleaching to confirm FRET in cells. Average FRET efficiency was 17.8 ± 3.0% ($n = 10$). A typical example is shown. ***B***, Effect of Ca^{2+} ionophore on FRET. FRET images of cells expressing wild-type Camuiα are shown to the right. Scale bar, 10 μm. $n = 12$. ***C***, Effect of the phosphatase inhibitor calyculin A (1 μM). Wild type (WT), $n = 4$; T286A, $n = 3$; T286D, $n = 5$. Images are shown in intensity-modulated display mode, in which a warmer hue indicates a higher CFP/YFP ratio or lower FRET and brightness indicates that of CFP channel using MetaMorph (Universal Imaging, West Chester, PA). Error bars represent SEM.

channels. After photobleaching of YFP, we observed a dequenching of the CFP signal, confirming FRET in intact cells (Fig. 3*A*). An application of the Ca^{2+} ionophore 4-Br-A23187 to the cells expressing Camuiα increased the CFP/YFP ratio, confirming the utility of Camuiα for monitoring CaMKII activation in living cells (Fig. 3*B*).

It has been shown that blockage of phosphatases alone is sufficient to increase the Ca^{2+}-independent activity of CaMKII (Strack et al., 1997). We therefore tested whether the phosphatase inhibitor calyculin A changes FRET by itself (Fig. 3*C*). Calyculin A induced a slow progressive increase in the CFP/YFP ratio in cells expressing wild-type Camuiα, which approached the level obtained by application of 4-Br-A23187. Additional application of 4-Br-A23187 did not produce any additional effects (data not shown), suggesting that both manipulations induced changes in FRET by a similar mechanism. In contrast, T286A mutant showed an attenuated response and T286D mutant started from a higher CFP/YFP ratio and did not show any additional change in FRET. Although this result itself may be explained by an increase in affinity to Ca^{2+}/calmodulin complex resulting from an increase in phosphorylation at T286 (Meyer et al., 1992), together with the biochemical studies described above, the results are consistent with the idea that FRET measurement detects autophosphorylation of CaMKII.

Imaging of Camuiα activation in neurons

We then expressed Camuiα in neurons in dissociated culture (Fig. 4). Camuiα was distributed along dendritic shafts and spines in fluorescent images (Fig. 4*A*). In unstimulated cells, the FRET level was relatively constant except for occasional changes in spines, possibly reflecting spontaneous synaptic activity (Fig. 4*B*,*C*). After stimulation with glutamate for 5 min, Camuiα was rapidly activated in both spines and dendrites, which was accom-

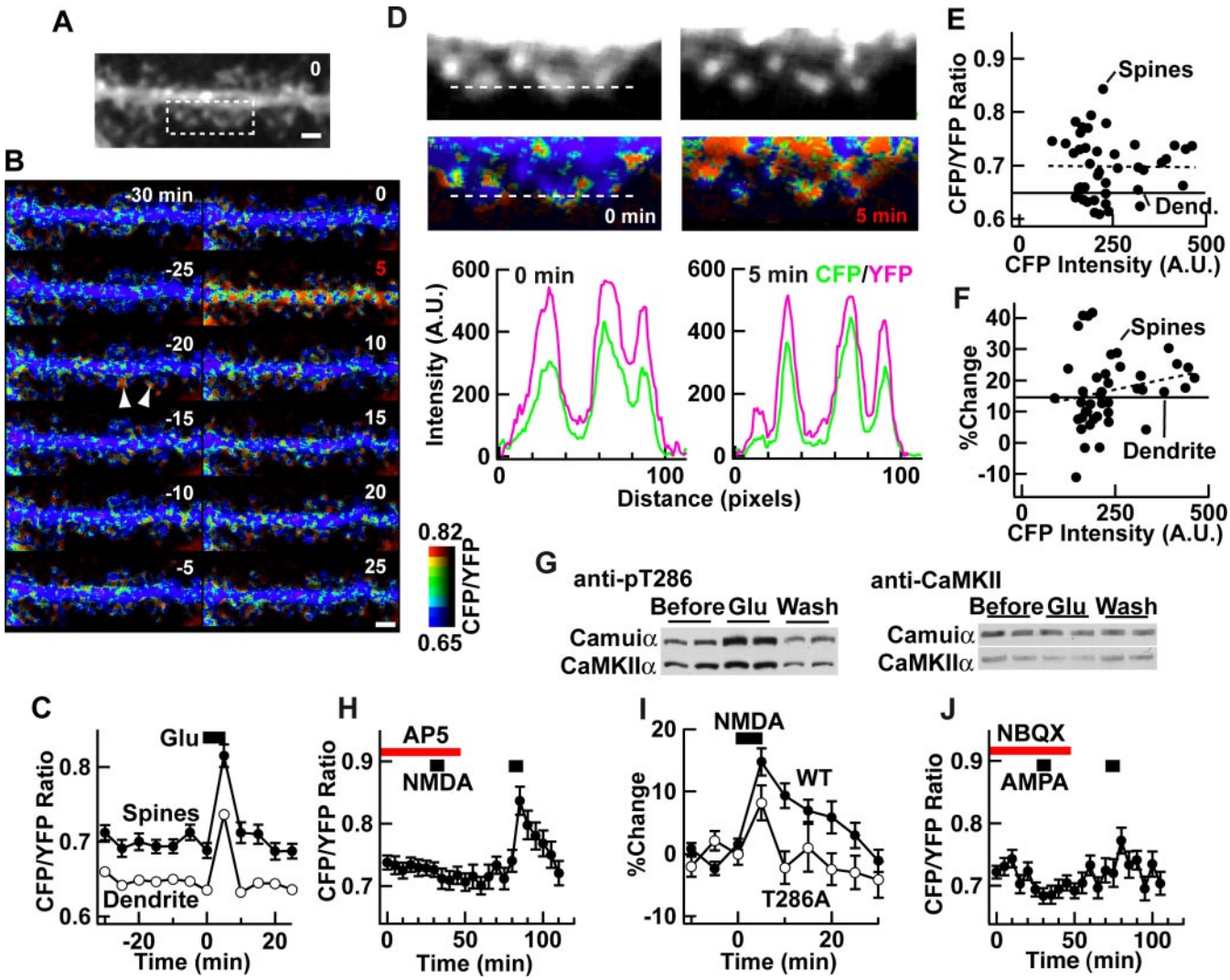

Figure 4. Detection of activation of synaptic Camuiα in hippocampal neurons. ***A***, An image of a neuron expressing Camuiα. ***B***, Time-lapse FRET images (intensity-modulated display mode) of the same neuron, stimulated with glutamate (20 μM) between time 0 and 5 min. Examples of spontaneous change are indicated by arrowheads. ***C***, Ensemble change in FRET level by glutamate application. FRET level in dendrites is also shown. There were 43 spines from two dendrites, one of which is shown in ***A*** and ***B***. ***D***, High-magnification images of the boxed area in ***A*** before and after stimulation. Graphs show background-subtracted CFP and YFP fluorescence profiles along a line (width, 5 pixels) across three spines. The background was 289.6 and 294.9 for CFP and 324.2 and 329.0 for YFP before and after the stimulation, respectively. A.U., Arbitrary units. ***E***, ***F***, Plots of unstimulated FRET level and glutamate-induced change versus unstimulated CFP intensity in individual spines. CFP intensity and unstimulated FRET level are the average of three images taken between −10 and 0 min. Dend., Dendrite. ***G***, Anti-phospho-T286 CaMKII and anti-CaMKIIα immunoblots of neurons similarly stimulated. Both Camuiα and endogenous CaMKIIα are shown. Experiments were done in duplicate. Glu, Glutamate; Wash, washout. ***H***, Effect of selective activation of NMDA receptor by NMDA (25 μM) and glycine (1 μM) (26 spines from 2 neurons). DL-AP-5 (100 μM) blocked the response. ***I***, Comparison of the NMDA receptor-mediated response of Camuiα wild-type (WT) and T286A mutant (60 spines from 4 neurons). ***J***, Effect of selective AMPA receptor activation with AMPA (40 μM) and blockade of effect with NBQX (1 μM; 28 spines from 2 neurons). ***H–J***, Experiments were performed in the presence of TTX (1 μM) to prevent secondary release of transmitters. Scale bars, 2 μm. Error bars represent SEM.

panied by redistribution, as described previously (Fig. 4*B–D*) (Shen and Meyer, 1999). This activation was reversible as it returned to the basal level after washout. We plotted basal FRET level, as well as glutamate-induced change versus fluorescence intensity in individual spines (Fig. 4*E*,*F*). This showed no strong correlation between the FRET level and fluorescence intensity, indicating a lack of correlation in both basal and stimulated CaMKII activity with the amount Camuiα that exists in each spine. In a parallel experiment, we blotted autophosphorylation of both Camuiα and endogenous CaMKII at T286 using anti-phospho-T286 CaMKIIα antibodies (Fig. 4*G*). The time courses of phosphorylation and FRET change were similar.

A selective activation of NMDA receptor by bath application of NMDA in the presence of glycine and TTX elicited FRET change as well, which could be blocked by the NMDA receptor antagonist DL-AP-5 (Fig. 4*H*). Under this condition, FRET change persisted for ~20 min after washout. In contrast, the T286A mutant showed a smaller response (~60% of wild type at the peak) and returned to baseline after washout (Fig. 4*I*). This shows that for FRET change to be persistent after the washout of NMDA, the autophosphorylation at T286 of Camuiα is required. Bath application of AMPA in the presence of TTX also elicited a FRET change that could be antagonized by 2,3-dihydroxy-6-nitro-7-sulfamoylbenzo[f]quinoxaline (NBQX), although the change is smaller (Fig. 4*J*).

Discussion

Here, we present the first FRET-based reporter for CaMKII activity, Camuiα, which detects the conformational change in CaMKII itself during the activation process. The conformational

change in CaMKII is supported by several lines of evidence (Mukherji et al., 1994; Bradshaw et al., 2002; Chin and Means, 2002), and our study unequivocally shows that CaMKII activation increases the distance between N and C termini of CaMKII and/or changes the angle between them. The analyses of mutants indicate that the binding of Ca^{2+}/calmodulin and the following autophosphorylation at T286 both contribute to the conformational change. Phosphorylation at other sites, including T305/T306 and S314, did not significantly contribute to the FRET change.

Our approach for detecting the conformational change in CaMKII itself as an index of CaMKII activation process is advantageous over a substrate-based FRET reporter, typically an optimal substrate for a kinase fused with a phosphoprotein-binding domain and flanked by CFP and YFP. The phosphorylation status of such a reporter will be affected by the phosphatase, in addition to the kinase, and therefore is likely to reflect a temporal summation of the balance of kinase and phosphatase activities in a given environment. By monitoring the conformational change in CaMKII itself, we expect that Camuiα more faithfully reflects CaMKII activity.

Using Camuiα in combination with two-photon microscopy, we could monitor autophosphorylation-dependent CaMKII activation in living neurons at single dendrite and spine resolution. Application of NMDA in combination with glycine evoked constitutive activation of CaMKII, which lasted ~20 min after washout. Currently, the prevailing model of synaptic plasticity is that CaMKII activity is constitutively maintained after the induction of synaptic plasticity, but the duration of activity and distribution of activated CaMKII are not clear. It would be intriguing to measure CaMKII activity using Camuiα and record synaptic responses. In addition, Camuiα may allow us to identify synapses undergoing synaptic potentiation, thereby serving as a useful tool to study the functional anatomy of local synaptic circuits. For instance, we may be able to express Camuiα in live animals using viral vectors or genetic methods and observe CaMKII activation while the animals are performing learning tasks. This will allow us to ascertain which synapse in a given cell or synaptic circuit is responsible for a particular learning process. Camuiα will thus provide important information about the learning process in an unprecedented way.

References

Bradshaw JM, Hudmon A, Schulman H (2002) Chemical quenched flow kinetic studies indicate an intraholoenzyme autophosphorylation mechanism for Ca^{2+}/calmodulin-dependent protein kinase II. J Biol Chem 277:20991–20998.

Brickey DA, Bann JG, Fong YL, Perrino L, Brennan RG, Soderling TR (1994) Mutational analysis of the autoinhibitory domain of calmodulin kinase II. J Biol Chem 269:29047–29054.

Carlezon Jr WA, Haile CN, Coppersmith R, Hayashi Y, Malinow R, Neve RL, Nestler EJ (2000) Distinct sites of opiate reward and aversion within the midbrain identified using a herpes simplex virus vector expressing GluR1. J Neurosci 20:RC62(1–5).

Chin D, Means AR (2002) Mechanisms for regulation of calmodulin kinase IIα by Ca^{2+}/calmodulin and autophosphorylation of threonine 286. Biochemistry 41:14001–14009.

Colbran RJ (1993) Inactivation of Ca^{2+}/calmodulin-dependent protein kinase II by basal autophosphorylation. J Biol Chem 268:7163–7170.

De Koninck P, Schulman H (1998) Sensitivity of CaM kinase II to the frequency of Ca^{2+} oscillations. Science 279:227–230.

Elgersma Y, Fedorov NB, Ikonen S, Choi ES, Elgersma M, Carvalho OM, Giese KP, Silva AJ (2002) Inhibitory autophosphorylation of CaMKII controls PSD association, plasticity, and learning. Neuron 36:493–505.

Fukunaga K, Muller D, Miyamoto E (1995) Increased phosphorylation of Ca^{2+}/calmodulin-dependent protein kinase II and its endogenous substrates in the induction of long-term potentiation. J Biol Chem 270:6119–6124.

Goldberg J, Nairn AC, Kuriyan J (1996) Structural basis for the autoinhibition of calcium/calmodulin-dependent protein kinase I. Cell 84:875–887.

Hayashi Y, Shi SH, Esteban JA, Piccini A, Poncer JC, Malinow R (2000) Driving AMPA receptors into synapses by LTP and CaMKII: requirement for GluR1 and PDZ domain interaction. Science 287:2262–2267.

Hudmon A, Schulman H (2002) Neuronal Ca^{2+}/calmodulin-dependent protein kinase II: the role of structure and autoregulation in cellular function. Annu Rev Biochem 71:473–510.

Katoh T, Fujisawa H (1991) Autoactivation of calmodulin-dependent protein kinase II by autophosphorylation. J Biol Chem 266:3039–3044.

Lisman J, Schulman H, Cline H (2002) The molecular basis of CaMKII function in synaptic and behavioural memory. Nat Rev Neurosci 3:175–190.

Meyer T, Hanson PI, Stryer L, Schulman H (1992) Calmodulin trapping by calcium-calmodulin-dependent protein kinase. Science 256:1199–1202.

Miyawaki A, Llopis J, Heim R, McCaffery JM, Adams JA, Ikura M, Tsien RY (1997) Fluorescent indicators for Ca^{2+} based on green fluorescent proteins and calmodulin. Nature 388:882–887.

Mukherji S, Soderling TR (1994) Regulation of Ca^{2+}/calmodulin-dependent protein kinase II by inter- and intrasubunit-catalyzed autophosphorylations. J Biol Chem 269:13744–13747.

Mukherji S, Brickey DA, Soderling TR (1994) Mutational analysis of secondary structure in the autoinhibitory and autophosphorylation domains of calmodulin kinase II. J Biol Chem 269:20733–20738.

Nagai T, Ibata K, Park ES, Kubota M, Mikoshiba K, Miyawaki A (2002) A variant of yellow fluorescent protein with fast and efficient maturation for cell-biological applications. Nat Biotechnol 20:87–90.

Okamoto K, Nagai T, Miyawaki A, Hayashi Y (2004) Rapid and persistent modulation of actin dynamics regulates postsynaptic reorganization underlying bidirectional plasticity. Nat Neurosci 7:1104–1112.

Ouyang Y, Kantor D, Harris KM, Schuman EM, Kennedy MB (1997) Visualization of the distribution of autophosphorylated calcium/calmodulin-dependent protein kinase II after tetanic stimulation in the CA1 area of the hippocampus. J Neurosci 17:5416–5427.

Renger JJ, Egles C, Liu G (2001) A developmental switch in neurotransmitter flux enhances synaptic efficacy by affecting AMPA receptor activation. Neuron 29:469–484.

Shen K, Meyer T (1999) Dynamic control of CaMKII translocation and localization in hippocampal neurons by NMDA receptor stimulation. Science 284:162–166.

Shi SH, Hayashi Y, Petralia R, Zaman S, Wenthold R, Svoboda K, Malinow R (1999) Rapid spine delivery and redistribution of AMPA receptors after synaptic NMDA receptor activation. Science 284:1811–1816.

Strack S, Choi S, Lovinger DM, Colbran RJ (1997) Translocation of autophosphorylated calcium/calmodulin-dependent protein kinase II to the postsynaptic density. J Biol Chem 272:13467–13470.

Zhang J, Campbell RE, Ting AY, Tsien RY (2002) Creating new fluorescent probes for cell biology. Nat Rev Mol Cell Biol 3:906–918.